Substantial organic impurities at the surface of synthetic ammonium sulfate particles

Junteng Wu, Nicolas Brun, Juan Miguel González-Sánchez, Badr R'Mili, Brice Temime Roussel, Sylvain Ravier, Jean-Louis Clément, Anne Monod

Atmos. Meas. Tech., 15, 3859–3874, 2022
https://doi.org/10.5194/amt-15-3859-2022

Atmospheric Measurement Techniques
Open Access
EGU

Substantial organic impurities at the surface of synthetic ammonium sulfate particles

Junteng Wu[1], Nicolas Brun[1], Juan Miguel González-Sánchez[1], Badr R'Mili[1], Brice Temime Roussel[1], Sylvain Ravier[1], Jean-Louis Clément[2], and Anne Monod[1]

[1]Aix Marseille Univ, CNRS, LCE, Marseille, France
[2]Aix-Marseille Univ, CNRS, ICR, Marseille, France

Correspondence: Junteng Wu (junteng.wu@univ-amu.fr) and Anne Monod (anne.monod@univ-amu.fr)

Received: 12 October 2021 – Discussion started: 24 November 2021
Revised: 28 March 2022 – Accepted: 1 May 2022 – Published: 29 June 2022

Abstract. Ammonium sulfate (AS) particles are widely used for studying the physical–chemistry processes of aerosols and for instrument calibrations. Small quantities of organic matter can greatly influence the studied properties, as observed by many laboratory studies. In this work, monodisperse particles (200–500 nm aerodynamic diameter) were generated by nebulizing various AS solutions and organic impurities were quantified relative to sulfate using a high-resolution time-of-flight aerosol mass spectrometer (HR-ToF-AMS). The organic content found in AS solutions was also tentatively identified using a liquid chromatography–tandem mass spectrometer (LC–MS). The results from both analytical techniques were consistent and demonstrated that the organic impurities contained oxygen, nitrogen, and/or sulfur, their molecular masses ranged from m/z 69 to 420, and they likely originate from the commercial AS crystals. For AS particle sizes ranging from 200 to 500 nm, the total mass fraction of organic compounds (relative to sulfate) ranged from 3.8 % to 1.5 %, respectively. An inorganic–organic mixture model suggested that the organic impurities were coated on the AS particle with a surface density of 1.1×10^{-3} g m^{-2}. A series of tests were performed to remove the organic content (using pure N_2 in the flow, ultrapure water in the solutions, and very high AS quality), showing that at least 40 % of the organic impurities could be removed. In conclusion, it is recommended to use AS seeds with caution, especially when small particles are used, in terms of AS purity and water purity when aqueous solutions are used for atomization.

1 Introduction

Atmospheric aerosols are generally a complex mixture of inorganic and organic compounds that have a strong impact on climate and human health (IPCC, 2013; Pöschl and Shiraiwa, 2015). According to the annual aerosol emission inventories, inorganic compounds account for the majority of the mass (Andreae and Rosenfeld, 2008). Among them, ammonium sulfate (AS) is considered as one of the dominant components (Charlson et al., 1992; Seinfeld et al., 2016). Because AS plays important roles in physical and chemical atmospheric processes, it has been extensively used in laboratory experiments to understand and reproduce these processes. In the past 20 years, more than 200 articles have been published using AS as (seed) particles for the study of optical properties, hygroscopic properties, phase transition and viscosity, as well as chemical reactivity of aerosols (see the detailed references in Sect. S1 in the Supplement). In all these studies, it was shown that the presence of organic matter, even at very low concentrations in AS particles, greatly influences these properties.

Among these studies, the study of aerosol hygroscopic properties represents the major contribution (115 papers out of the 219 cited in Sect. S1). Ammonium sulfate aerosols are very often chosen as seed particles to study hygroscopic behavior of mixed organic–inorganic aerosols. Scanning various conditions of temperature and relative humidity (RH), hygroscopicity properties of aerosols were investigated via measurements of hygroscopic growth, cloud condensation nuclei (CCN) activity, and ice nuclei (IN) activity. It is well established that the hygroscopic parameter kappa (κ)

of pure AS particles is 0.53 [0.33–0.72] and 0.61 according to the growth factor derivation and the CCN derivation, respectively (Clegg et al., 1998; Koehler et al., 2006; Petters and Kreidenweis, 2007). Laboratory studies show that the hygroscopic behavior of most water soluble inorganic mixed aerosols is additive in nature, i.e., following the ZSR (Zdanovskii, Stokes, and Robinson) assumption (Stokes and Robinson, 1966). However, when organic compounds are present in AS aerosols, their hygroscopic properties are more complex. Firstly, for water soluble organic compounds such as short carbon chain (di)carboxylic acids, their effects on AS aerosols are represented by their hygroscopicity and mass fraction suggested by the ZSR assumption (Abbatt et al., 2005; Brooks et al., 2004; Hämeri et al., 2002; Prenni et al., 2003). Secondly, for less soluble compounds and complex mixtures, their solubility significantly influences the hygroscopic behavior of AS aerosol. At sub-saturation conditions, secondary organic aerosol (SOA) formed on AS seed particles from α-pinene photo-oxidation lowers the hygroscopic growth factor (HGF) of AS (Meyer et al., 2009). Specifically, at RH below the deliquescence point, AS seeded SOA do not follow the ZSR predictions because the solutions are highly concentrated and thus non-ideal. When the insoluble organic compounds are the dominant components of the aerosol, the water uptake on organic AS particles is significantly slowed down and requires a longer residence time to achieve thermodynamic equilibrium (Sjogren et al., 2007). The same behavior has also been observed at super-saturation conditions, i.e., the thick coating of insoluble organics compounds, such as stearic acids, act as a shield preventing the interaction of AS and water, thus suppressing AS hygroscopicity (Abbatt et al., 2005). Thirdly, it was found that organic compounds could affect the hygroscopicity of AS by lowering the surface tension, such as marine organic compounds at low concentrations (Moore et al., 2008), or ozonolysis products of monoterpenes (King et al., 2009; Wex et al., 2009; Engelhart et al., 2008). It has been shown that atmospheric surfactants could reduce the aerosol surface tension by a factor of 2 compared with water surface tension (72 mN m^{-1}) (Gérard et al., 2019; Nozière et al., 2014; Sorjamaa et al., 2004). The presence of small amounts of surface-active organic compounds may reduce the aerosol surface tension, affecting its hygroscopic properties: according to some models, a 10 % reduction in the surface tension results in a 30 % increase in the hygroscopic parameter κ (Ovadnevaite et al., 2017; Petters and Kreidenweis, 2013). More recently, several models have shown that the inferred behavior of the surface tension strongly depends on the selected modeling approach (Prisle, 2021; Vepsäläinen et al., 2022). In conclusion, organic compounds can have a very complex impact on the hygroscopic growth and CCN activity of aerosol particles which may go beyond the simple reduction of the value of a single parameter in the Köhler equation, and numerous models are currently under development on this issue.

Ammonium sulfate has also been widely used to understand the phase transition of organic–inorganic compounds in single particles studies (49 papers out of the 219 cited in Sect. S1). Under sub-saturated conditions, deliquescence of pure AS occurs at $\sim$ 80 % RH and efflorescence at $\sim$ 34 % RH. However, these phase transition behaviors of AS particles are significantly influenced by organic compounds. For example, the presence of humic acids decreases the deliquescence RH and increases the efflorescence RH of AS aerosols (Badger et al., 2006). Furthermore, the presence of malonic acid on AS particle leads to a two-step deliquescence instead of a single step in the hygroscopic growth (Treuel et al., 2009). Differently to the shift in deliquescence RH and/or efflorescence RH, the presence of SOA completely removes the clear phase transition of AS on the particle: this was clearly shown for SOA derived from cycloalkene photolysis and monoterpenes photo-oxidation (Varutbangkul et al., 2006). The change in phase transition behavior of AS particles also depends on the quantity of organic compounds. During the hygroscopic growth, for small organic or inorganic ratios (< 20 %), there is a bulk-to-surface partitioning with a part of the organic material in the solution, and another part as a film coated at the surface of the droplet (Nandy and Dutcher, 2018; Smith et al., 2013), while high organic or inorganic ratios (> 80 %) induce liquid–liquid phase separation (Smith et al., 2013; Saukko et al., 2015).

Due to their hygroscopic properties, AS aerosols easily provide an aqueous environment, where reactions between NH_4^+, SO_4^{2-}, and water-soluble organic compounds can play an important role in the formation of secondary aerosols (62 papers among the 219 cited in Sect. S1). Some of these reactions may explain the source of the so-called brown carbon, thus affecting the optical properties of particles (44 papers among the 219 cited in Sect. S1). Ammonium cations (NH_4^+) are in a pH-dependent equilibrium with dissolved ammonia in the aqueous phase. NH_3 can react with carbonyl compounds such as glyoxal, methylglyoxal, glycolaldehyde, hydroxyacetone, biacetyl, or unsaturated dialdehydes in Maillard-type browning reactions to form light absorbing and oligomeric compounds such as imidazoles or pyrazine-based compounds (Hensley et al., 2021; Grace et al., 2020; Hawkins et al., 2018; Laskin et al., 2014; Kampf et al., 2012). These reactions are of particular interest for the atmosphere, as they have an impact on both health and climate. Their aqueous-phase processes represent an important and rapid source of brown carbon (Powelson et al., 2014; De Haan et al., 2017; Jimenez et al., 2022). In addition, SO_4^{2-} is not inert in atmospheric water. Sulfate anions can react with •OH radicals forming sulfate radicals ($SO_4^{\bullet-}$), an important atmospheric oxidant (Herrmann, 2003). Besides, sulfate radicals contribute to the formation of organosulfates (Nozière et al., 2010; Brüggemann et al., 2020; Wach et al., 2019; Szmigielski, 2016). Organosulfates are ubiquitous compounds in SOA with important implications in their physicochemical properties (Shakya and Peltier,

2015). Other chemical pathways that lead to the formation of organosulfates might involve directly sulfate anions, i.e., their nucleophilic substitution to epoxides or tertiary nitrates (Hu et al., 2011; Darer et al., 2011), and the acid-catalyzed esterification of alcohol groups (Surratt et al., 2008; Linuma et al., 2007).

Due to the atmospheric representativity of AS particles and their well-known physical and chemical properties, they are often chosen as a reference in aerosol studies, as mentioned above, and for instrumentation calibration. The presence of trace organic compounds in AS particles may induce potentially important artifacts on the experimental results of physical and chemical processes. Few laboratory studies show that organic compounds can be present in synthetic AS particles. For example, 0.8 wt % of C was observed in solutions where only ammonium sulfate was present as a solute in the study of phase transitions of AS (Badger et al., 2006). In another example, in a study of glyoxal uptake on AS particles monitored by an aerosol mass spectrometer, Trainic et al. (2011) found organic fragments on pure AS aerosols (purity not mentioned), with a ratio of organic matter to sulfate (hereafter named [Org] / [Sulfate]) as high as 8 %. Scanning the 219 articles (mentioned in Sect. S1 in the Supplement) published over the past 20 years using AS aerosols in the laboratory, it appears that neither quantification nor identification of these potential organic impurities were reported. Furthermore, the majority of these studies (63 %) did not mention the origin and purity of the AS used. As organic traces may significantly influence the properties of AS particles, and thus bias experimental results, the objectives of this work were to quantify organic traces in commercial AS under conditions used in laboratory experiments, and when possible, tentative identification was performed. Finally, recommendations are given for purity improvements.

2 Method

Ammonium sulfate aerosol particles were generated by atomization of AS solutions at concentrations ranging from 0.01 to 0.5 M. Ammonium sulfate aerosols were selected at four sub-micrometer sizes to test the effect of particle size on the organic content. This procedure allowed us to form quasi-monodisperse AS particles at mass concentrations ranging from 5 to 30 $\mu g\,m^{-3}$, concentrations typically used for aerosol generation and/or calibration in the literature. Their chemical composition was quantified online by a high-resolution time-of-flight aerosol mass spectrometer (HR-ToF-AMS). Additionally, aqueous solutions of AS were analyzed by liquid chromatography–tandem mass spectrometry (LC–MS) to tentatively identify organic content. All chemical compounds used in this work are listed in Sect. S2 in the Supplement.

2.1 Detection of organic traces in AS aerosol particles

2.1.1 Aerosol generation and size classification

The experimental setup for quantifying organic content is shown in Fig. 1. Aqueous solutions of AS (0.01–0.5 M) were nebulized by atomization (using a 3076 atomizer, TSI) that generated droplets with compressed air at 1 bar above atmospheric pressure and a flow rate of 1.8 $L\,min^{-1}$. As a comparison with compressed air, pure N_2 (Linde gas, 99.999 %) was used. The resulting droplets were dried by a Nafion™ dryer at relative humidity (RH) below 25 %, i.e., below the efflorescence of AS aerosol. Dry AS particles then passed through a dilution system aimed at controlling AS particle concentrations. It consisted of two parallel pathways, one of which was connected to a HEPA filter. An aerodynamic aerosol classifier (AAC, Cambustion) and an electrostatic classifier (3080, TSI) combined with a differential mobility analyzer (3081 long DMA) were alternatively used to select monodisperse particles. The ratio of air sheath flow to sample flow was fixed at 10 for the two classifiers. To regulate the flow rate through the AAC classifier, a mass flow controller (MFC) was connected to a vacuum pump. Under this configuration, the sample flow through the AAC varied from 0.4 to 1.4 $L\,min^{-1}$, while the tests performed with the DMA classifier were only done at one flow rate (0.4 $L\,min^{-1}$). This setup allowed the characterization of the aerosol particles by their sizes, as well as their organic content as a function of particle sizes with respect to the total mass of AS particles selected.

2.1.2 Experimental conditions for the investigation of AS aerosol particles

A series of experiments (Table 1) were performed to quantify organic content on AS aerosol particles by scanning various conditions of mass concentrations, particle size, and generation procedures. In this work, four different particle diameters were used: the mobility diameter (d_m), the aerodynamic diameter (d_a), and the vacuum aerodynamic diameter (d_{va}) were given by the SMPS, the AAC, and the AMS measurements, respectively; while the volume equivalent diameter (d_{ve}) was used to determine the surface of AS particle. The relations between these diameters were described by DeCarlo et al. (2004). As organic compounds can be homogenously mixed in AS aerosol or remain at the particle surface inducing different behavior as a function of size (Jimenez et al., 2009; Tervahattu et al., 2002), monodisperse AS particles were selected with aerodynamic size (d_a) varied from 200 to 500 nm in each experiment. In experiment P1 (EXP P1), AS crystals (99.5 %, for analysis, from Acros Organics™ Fisher Scientific) were dissolved in Milli-Q water (18.2 MΩ cm, TOC < 2 ppb) at various concentrations (0.01–0.5 M). In EXP P2–P7, the aqueous phase concentration of AS was fixed at the highest value (0.5 M) to study the influ-

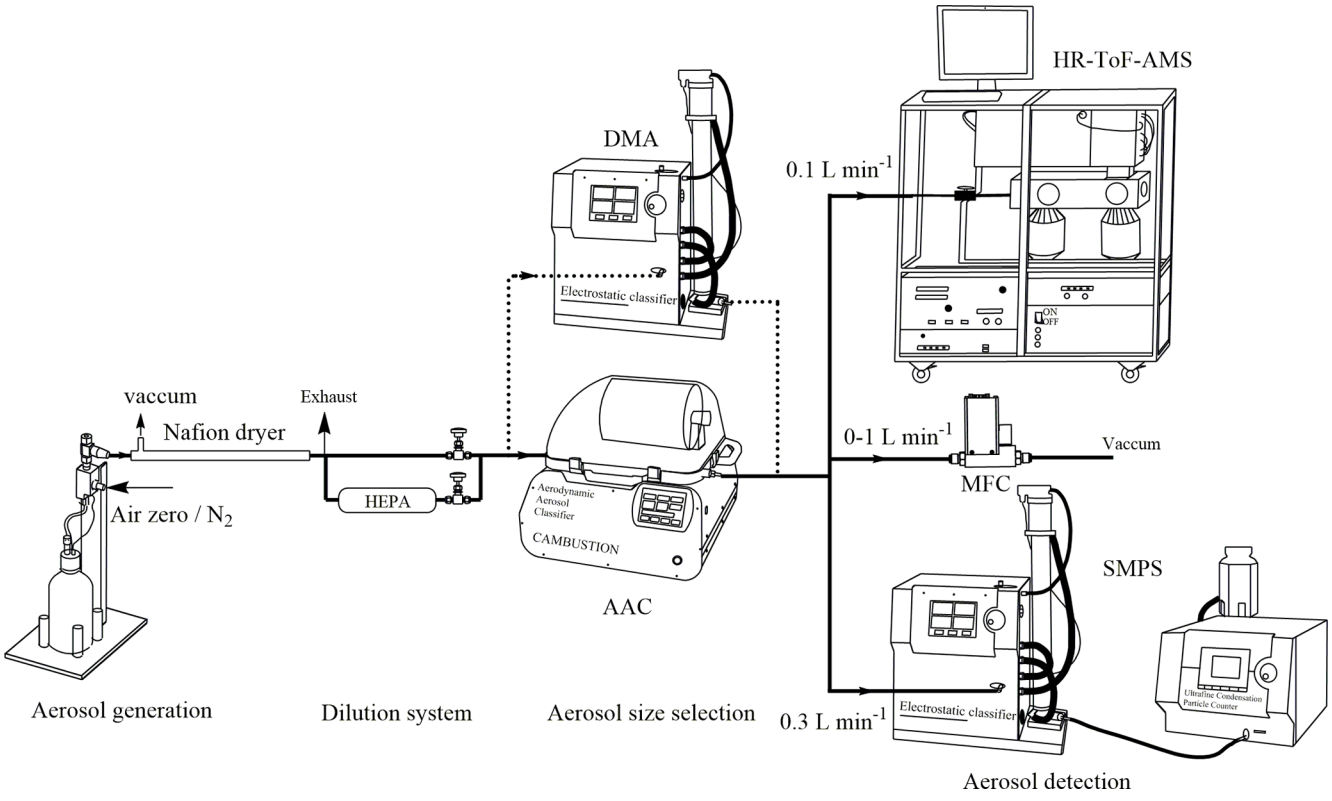

Figure 1. Experimental setup for the quantification of organic content in monodisperse ammonium sulfate particles.

ence of other parameters. In EXP P2, the influence of the water quality was tested. In EXP P3–P5, the influence of the purity of AS crystals was tested. In EXP P3, AS crystals (99.5 %, for analysis, from Acros Organics™ Fisher Scientific) were tentatively purified by an accelerated solvent extractor (ASE 300, Dionex) using acetonitrile as the extraction solvent. In EXP P4, AS crystals (99.5 %, for analysis, from Acros Organics™ Fisher Scientific) were tentatively purified by recrystallization in Milli-Q water: AS crystals (20 g) were dissolved into boiling water (20 mL) reaching a concentration of 7.5 M and then recrystallized by smooth cooling at room temperature. In EXP P5, high purity AS (99.9999 % Suprapur® from Merck) was used. In EXP P6, the influence of the particle size selector was studied by intercomparison between the DMA and the AAC. Developed by Tavakoli and Olfert (2013), the AAC is a recent commercial aerosol classifier which selects the particle size by centrifugal force instead of electrostatic force which is used in the DMA. In the AAC, the aerodynamic diameter of selected particles is related to the rotational speed of the concentric cylinder, the sheath flow rate, and the sample flow rate. Rotational speed has been reported to influence the geometric standard deviation (σ_{geo}) of size distribution, i.e., the higher the rotational speed, the smaller the size and the larger the σ_{geo} (Johnson et al., 2018). In EXP P7, the effect of the rotational speed of the concentric cylinder in the AAC was tested while maintaining a constant size selection by regulating the MFC (Fig. 1), so that the sample flow through the AAC varied from 0.4 to 1.4 L min^{-1}.

2.1.3 Characterization of aerosol particles

The particles number size distribution was measured with a scanning mobility particle sizer (SMPS) consisting of a DMA (3080, TSI) coupled with an ultrafine condensation particle counter (CPC, 3776, TSI). A high-resolution time-of-flight aerosol mass spectrometer (HR-ToF-AMS, Aerodyne Research) was used to measure the bulk chemical composition of non-refractory sub-micron particulate matter (DeCarlo et al., 2006). The instrument was used under standard conditions (standard vaporizer at 600–650 °C and electron ionization at 70 eV) in V mode and in p-ToF mode. Each measurement point was averaged for an MS cycle of 1 min and a p-ToF cycle of 30 s. Calibrations using pure and dried particles of ammonium nitrate and ammonium sulfate with a mobility diameter of 350 nm were carried out every few days of operation to determine the ionization efficiency of nitrate, ammonium, and sulfate named as IE_{NO_3}, RIE_{NH_4}, and RIE_{SO_4}. The RIE_{NH_4} and RIE_{SO_4} values were related to nitrate and were estimated experimentally as 3.3 and 1.8, respectively. The standard recommended value for RIE_{org} of 1.4 was used for organic compounds. Calibration in the p-ToF mode was carried out using pure ammonium

Table 1. Experiments to quantify organic traces on AS aerosol particles under various conditions: [1] AS 99.5 %, for analysis, from Acros Organics™ Fisher Scientific; [2] purification by solvent (acetonitrile) extraction; [3] purification by recrystallization; [4] AS 99.9999 % Suprapur® from Merck. [5] Milli-Q water, 18.2 MΩ cm, TOC < 2 ppb; and [6] Fisher Chemical, LC–MS grade. Under each condition, duplicate experiments were performed for each selected particle size. The four sizes ($d_a = 200$, 300, 400, and 500 nm) selected with the AAC classifier correspond to the mobility sizes ($d_m = 130$, 201, 269, and 336 nm).

Experiment	AS purity (%)	Water	AS liquid concentration (M)	Particle size (nm)
Size selection by the AAC (sample flow = 0.4 L min^{-1})				
P1	99.5[1]	Milli-Q[5]	0.01, 0.02, 0.05, 0.1, 0.2, 0.5	$d_a = 200, 300, 400, 500$
P2	99.5[1]	Fisher[6]	0.5	$d_a = 200, 300, 400, 500$
P3	99.5[1] purified[2]	Fisher[6]	0.5	$d_a = 200, 300, 400, 500$
P4	99.5[1] recryst[3]	Fisher[6]	0.5	$d_a = 200, 300, 400, 500$
P5	99.9999[4]	Fisher[6]	0.5	$d_a = 200, 300, 400, 500$
Size selection by the DMA (sample flow = 0.4 L min^{-1})				
P6	99.5[1]	Milli-Q[5]	0.5	$d_m = 122, 188, 250, 311, 375$
Size selection by the AAC (sample flow = 0.5, 1.0, 1.4 L min^{-1}, corresponding to a rotation speed of 190, 285, and 369 rad s^{-1})				
P7	99.5[1]	Milli-Q[5]	0.5	$d_a = 300$
Effect of gas supplier (pure N_2 instead of compressed air)				
P8	99.5[1]	Milli-Q[5]	0.5	$d_a = 200, 300, 400, 500$

nitrate in the size range of 80–500 nm mobility diameter. The data treatment has been performed with AMS Analysis Toolkit 1.63 and PIKA 1.23 under the software Igor Pro 6.37. The selection of ions to fit in PIKA was derived from the mass spectra produced by AS aerosols at $d_a = 200$ nm in EXP P1 and was rechecked in each experiment. To avoid any overestimation of the organic fraction, CHO^+ and CO_2^+ fragments (at m/z 29 and 44) were corrected from the remaining gas phase in the AMS (Aiken et al., 2007; Canagaratna et al., 2015). In addition, due to the very high signals of the fragments NH_x and SO_x, other fragments located at the tail of these main peaks (such as CH_3^+, CH_4^+, CH_2N^+, $C_2H_4^+$ ...) were excluded from the calculation of the total organic content to avoid any overestimation of the organic fraction.

2.2 Seeking for organic traces in AS aqueous solutions

The characterization of organic traces on AS aerosol particles were also investigated directly in AS aqueous solutions using a liquid chromatography–tandem mass spectrometer (LC–MS) for tentative molecular identification. The system comprised a liquid chromatograph (Acquity system, Waters) coupled with quadruple-time-of-flight mass spectrometer (Synapt G2 HDMS, Waters) fitted with an electrospray ion source (ESI). The chromatographic separation was carried out on an Atlantis T3 reversed phase C18 column (100 × 2.1; 3 µm, Waters), the mobile phase consisted of two eluents: eluent A was Milli-Q water (resistivity 18 MΩ cm at 25 °C) with 0.1 % formic acid, and eluent B was either methanol (Optima© LC/MS grade, Fisher Scientific) with 0.1 % formic acid or acetonitrile (Fisher Chemical, Optima © LC/MS grade) with 0.1 % acid. The gradient elution was performed at a flow rate of 0.4 mL min^{-1} using 5 % of (B) held 1 min and 5 %–95 % of (B) within 5 min. The sample injection volume was 5 µL. In the ESI, the capillary voltage was set to 1 kV, the desolvation gas flow was 1000 L h^{-1} at 500 °C, and the source temperature was 150 °C. During each chromatographic run, leucine enkephalin (2 ng µL^{-1}, $C_{28}H_{37}N_5O_7$, molecular weight 555.27 g mol^{-1}, Sigma-Aldrich) was used as internal standard to perform mass correction. The mass spectrometer was tuned to V mode with a resolving power of 18 000 at m/z 400 and allowed the determination of elemental composition with a mass accuracy lower than 5 ppm. For elemental attribution, the ranges of atom number were set as follows: C [0–30], H [0–60], N [0–5], O [0–10], S [0–3], P [0–3], and Na [0–1], thus covering the most common elements (Kind and Fiehn, 2007). An isotope prediction algorithm, based on the mass of the molecular ion and the relative intensity of the first and second isotopes, was applied to reduce the number of proposed elemental compositions. Data were collected from 50 to 600 Da in the positive and negative ionization modes. All products were detected as their protonated molecules ($[M+H]^+$) or sodium adducts ($[M+Na]^+$) in the positive mode, and their deprotonated molecules ($[M-H]^-$) in the negative mode. In some experiments, complementary analyses were performed using MS/MS fragmentation with various collision energies.

Table 2. Experiments of characterization of organic traces in AS liquid solutions. The elution gradient and ESI setup were the same for all experiments: [1] AS 99.5 %, for analysis, from Acros Organics™ Fisher Scientific; [2] AS 99.5 % EMSURE® from Merck; [3] eluents: A = H_2O with 0.1 % formic acid, and B as specified; [4] acetonitrile, [5] methanol, [6] methyl tert-butyl ether, [7] dichloromethane; L–L: liquid–liquid, S–L: solid–liquid.

Experiment	Type of experiment				LC–MS analytical conditions	
	AS purity (%)	AS aqueous concentration	Sample preparation	Extracting solvent	Eluent B[3]	MS mode
C1	99.5[1]	1.5 M	None	–	ACN[4] 0.1 % acid	ESI^+–MS/ESI^-–MS
C2					MeOH[5] 0.1 % acid	
C3			L–L extraction	MTBE[6]	ACN[4] 0.1 % acid	ESI^+–MS/ESI^-–MS
C4				DCM[7]		
C5				ACN[4]		
C6		2.5 M				
C7		crystals	S–L extraction		MeOH[5] 0.1 % acid	
C8	99.5[2]					
C9	99.5[1]	5 M	L–L extraction			ESI^+-MS–MS
C10	99.5[2]	5 M	L–L extraction			ESI^+–MS/ESI^-–MS

Although the organic purity is not mentioned on commercial crystals (only the inorganic content is indicated), two different brands of AS of the same purity were analyzed to seek for potential organic traces and for comparison purposes: one from Acros Organics™ Fisher Scientific (99.5 %, for analysis) that has been widely used in the literature, and EMSURE® from Merck (99.5 %, for analysis). The characterization experiments are shown in Table 2; each one was systematically complemented by blank experiments, i.e., analysis of the water used for each AS solution.

In EXP C1 and C2, aqueous solutions of AS were injected into the LC–MS, and two elution solvents were tested to optimize the chromatographic separation. In EXP C3–C10, organic compounds were extracted from AS crystals by different methods (solid–liquid and liquid–liquid extraction) using various solvents, and pre-concentrated prior LC–MS analysis using both positive and negative modes. For these extractions, an accelerated solvent extractor (ASE 300, Dionex) system was used under the following conditions: acetonitrile was the extraction solvent, the oven was set at 100 °C under 100 bars, the heat-up time and static time were 5 min each, and three extraction cycles were conducted. As an extension of EXP C6, EXP C9 was designed to perform MS/MS analysis using very high concentrations of AS to optimize the identification of organic traces, and analyses were performed in the positive mode only. For comparison purposes, another brand of AS of the same purity (99.5 %) was used in EXP C8 and C10 using two extraction methods.

3 Results and discussion

3.1 Organic content on AS aerosol particles

A significant quantity of organic matter was directly observed by the HR-ToF-AMS in EXP P1. As an example, Fig. 2 shows the mass concentrations of total organic matter and sulfate and their ratios as a function of time during one size cycle performed in EXP P1 at AS concentration of 0.01 M. Figure 2 also provides background signals obtained with the two pure waters of different qualities used in EXP P1 and P2. In these background signals, the total mass concentrations of organic compounds and sulfate are 0.018 ± 0.009 and $0.002 \pm 0.001\ \mu g\ m^{-3}$, respectively, similar to the detection limits of the HR-ToF-AMS in the V mode (DeCarlo et al., 2006). In the presence of AS, a significant quantity of organic compounds was observed with concentrations ranging from 0.15 to $0.33\ \mu g\ m^{-3}$ when the aerodynamic size of the particle varied from 500 to 200 nm, with a very good reproducibility in the duplicate experiments, at each size. Furthermore, the evolution of the mass ratio between total organic compounds and sulfate marked as [Org] / [Sulfate] (Fig. 2) shows a clear correlation with particle size: this ratio increases when the particle size decreases. The same observations were obtained at all other AS concentrations investigated in EXP P1 and in the other experiments. It was checked in EXP P8 that when replacing compressed air by pure N_2 (Linde Gas, 99.999 %), no significant differences were observed from EXP P1 under the same conditions (Sect. S3 in the Supplement). Overall, it was observed that

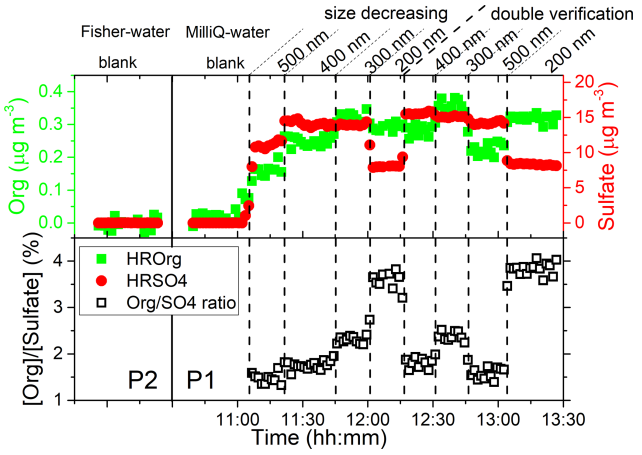

Figure 2. Mass concentrations of total organic matter, sulfate, and [Org] / [Sulfate] ratio as a function of time during one cycle performed in EXP P1 at an AS concentration of 0.01 M. Background signal obtained with pure water in EXP P1 and P2 is also shown for quality check and for comparison between the two types of water with different purity.

[Org] / [Sulfate] varied from 1.5 % to 3.8 %, in the range of the values reported by studies mentioning the presence of organic compounds in laboratory experiments on AS particles (0.8 wt % of C in Badger et al., 2006, and up to 8 % in Trainic et al., 2011).

The total mass concentration of organic compounds was calculated based on all organic fragments, as described in the previous Sect. 2.1.3. Figure 3 shows the unit-mass resolution spectrum of AS aerosols selected by the AAC at $d_a = 200$ nm.

SO_x and NH_x families represent sulfate and ammonium, respectively. All the other fragments are between 1 and 3 orders of magnitude lower, but detectable signals span for m/z up to 100. The sum of the signals of NO_2^+ and NO^+ fragments represent 30 % of the total organic signal (Fig. S4-1 in the Supplement). To figure out the source of this non-negligible nitrate signal, the AMS signal NO_2^+ / NO^+ ratio was investigated and showed significantly lower values in AS aerosol (0.46 in EXP1) compared with ammonium nitrate particles used for calibration (1.18) (Fig. S4-2 in the Supplement). It is thus suggested that the observed nitrate signal in AS aerosol is due to the presence of organic nitrates (Kiendler-Scharr et al., 2016). Concerning organic fragments, significant signals were observed for fragments $C_xH_y^+$ at m/z 27, 39, 41, 43, 55, 57, 67, and 69, for $C_xH_yO^+$ at m/z of 28 and 30, for $C_xH_yO_2^+$ at m/z 44, and for $C_xH_yN^+$ at m/z 30, 58, 72, and 86. (Raw spectra of CHN fragments are shown in Sect. S5 in the Supplement.) The potential "Pieber effect" was also investigated to elucidate any positive artifact on the determined quantities of organic compounds. Indeed, Pieber et al. (2016) showed that inorganic salts like AS or ammonium nitrate can trigger the CO_2^+ signal (m/z 44) due to reactions on the vaporizer of the AMS instrument. In the present study, the observed CO_2^+ signal represented 20 ± 5 % of the total organic signal. Thus, if all the CO_2^+ fragments came from the interference signal of sulfate, the maximum Pieber effect in this work would be 0.76 % relative to sulfate. It was thus not considered in the results. The rest of the organic fragments seem to represent organic molecules bearing various functionalities, potentially comprising oxygen and nitrogen. Before further identification of these compounds, Sects. 3.2 and 3.3 present the results and discussions on the influence of the particle size and liquid AS concentrations on the organic content.

3.2 The role of particle size and liquid AS concentrations on the quantity of organic content

Figure 4 shows [Org] / [Sulfate] measured in AS aerosols at various nebulized solution concentrations as a function of particle size. While no significant influence of AS aqueous phase concentration has been found (within experimental uncertainty), a significant influence of particle size is clearly observed on [Org] / [Sulfate].

To further understand how the organic matter was mixed with AS aerosols, two series of calculations were performed, following two hypotheses on the organic–inorganic mixing: (i) organic coating on the surface of monodisperse AS particles, and (ii) internal mixing. To achieve this calculation, a thorough study of the morphology of AS particles was performed using the various size measurements (Appendix A). For monodisperse AS particles selected by the AAC at a required aerodynamic diameter (d_a), its mobility diameter (d_m) and vacuum aerodynamic diameter (d_{va}) were measured by SMPS and HR-ToF-AMS, respectively.

The calculations of [Org] / [Sulfate] using each of these two hypotheses are detailed hereafter:

– *Hypothesis 1*: AS aerosols were coated by organic compounds with a size-independent surface density $\rho_{org,S}$ (in g m^{-2}).

For a non-spherical particle, the total surface of the particle was considered as the surface of the volume equivalent particle. According to DeCarlo et al. (2004), the relation between the volume equivalent diameter (d_{ve}) and $d_a$is described as Eq. (1):

$$d_a = d_{ve}\sqrt{\frac{\rho_p}{\rho_0}\frac{1}{\chi}\frac{C_c(d_{ve})}{C_c(d_a)}}, \quad (1)$$

where χ is the shape factor of aerosol particles and C_c is the Cunningham slip factor (Kim et al., 2005), given by Eq. (2):

$$C_c(K_n) = 1 + K_n\left[1.165 + 0.483\exp\left(-\frac{0.997}{K_n}\right)\right]. \quad (2)$$

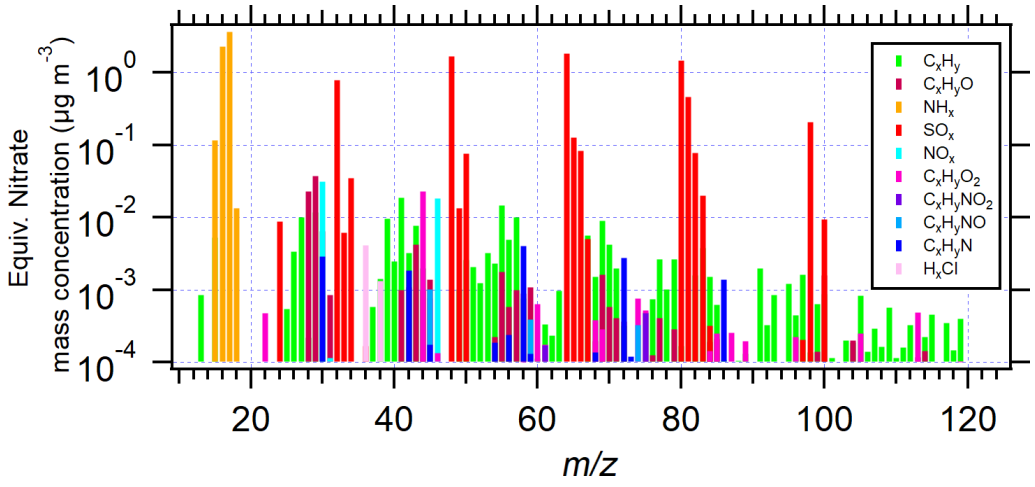

Figure 3. Unit-mass resolution spectra (averaged over 12 measurements, converted from the high-resolution data) of AS aerosol particles ($d_a = 200$ nm) in EXP P1, performed at an AS concentration of 0.5 M.

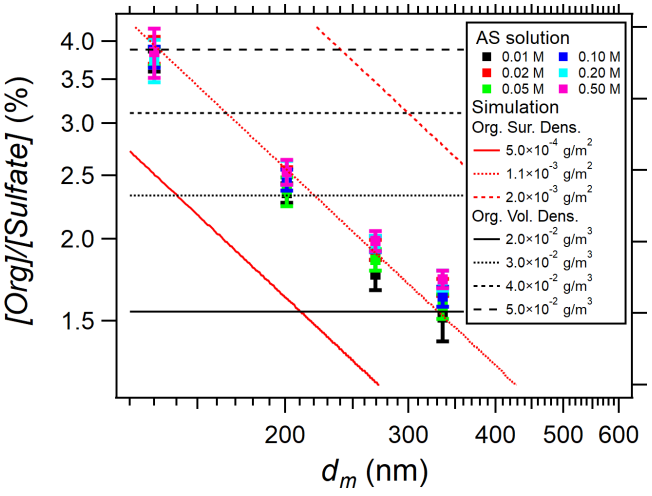

Figure 4. [Org] / [Sulfate] in AS aerosols versus particle mobility size (d_m) during EXP P1 scanning the six nebulized AS concentrations (0.01–0.5 M). The colored dots (with error bars) are the experimental data, while the red and black lines represent the calculated [Org] / [Sulfate] considering either surface coating of organic matter (in red from Eq. 3) or internal mixing (in black from Eq. 4).

$K_n(d) = 2\lambda_g/d$ is the Knudsen number, and λ_g is the gas mean free path. In this work, d_a was given by the AAC; χ was determined by d_m and d_{va} (Appendix A). Normal temperature and pressure (293.15 K at 1 atm) were applied for the calculation of d_{ve}. The surface of AS particles was estimated from the value of d_{ve}. Therefore, the prediction of surface coated organic compounds compared with sulfate mass is described in Eq. (3):

$$\frac{[\text{Org}]}{[\text{Sulfate}]} = \frac{\rho_{\text{org},S} S_{ve}}{V_{ve}\rho_{AS}\frac{M_{SO_4}}{M_{AS}}} = \frac{3}{2}\frac{\rho_{\text{org},S}}{d_{ve}\rho_{AS}\frac{M_{SO_4}}{M_{AS}}} \times 100\,\%, \quad (3)$$

where S_{ve} and V_{ve} are the surface and volume of the volume equivalent AS particle, respectively. M_{SO_4} and M_{AS} are molar mass of SO_4^{2-} and $(NH_4)_2SO_4$, respectively. [Org] and [Sulfate] are the mass concentrations of organic compounds and of sulfate in the particulate phase. Equation (3) shows that, in this case, [Org] / [Sulfate] decreases when the particle size increases.

– *Hypothesis 2*: Organic compounds are homogeneously mixed in AS aerosols with a density $\rho_{\text{org},V}$ (in g m^{-3}).

In this case, the mass concentration of organic compounds compared with sulfate is described by Eq. (4):

$$\frac{[\text{Org}]}{[\text{Sulfate}]} = \frac{V\rho_{\text{org},V}}{V\rho_{AS}\frac{M_{SO_4}}{M_{AS}}} = \frac{\rho_{\text{org},V}}{\rho_{AS}\frac{M_{SO_4}}{M_{AS}}} \times 100\,\%, \quad (4)$$

where V is the total volume of the studied aerosol particle. In this case, [Org] / [Sulfate] is independent of the particle size.

The results of these two calculations are shown in Fig. 4 together with the experimental results. The comparison clearly shows that the organic compounds coat homogenously on the surface of AS particles with a surface density of 1.1×10^{-3} g m^{-2}. In addition, this result shows that the Nafion™ dryer was not efficient in removing these organic compounds, probably due to their low volatility.

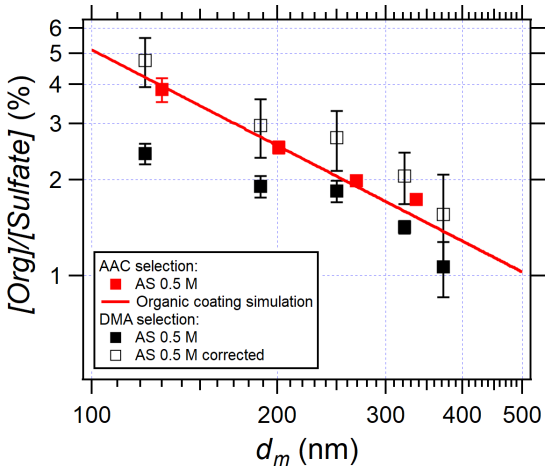

Figure 5. Influence of instrumental conditions and instrument intercomparison: AAC selection (red squares, EXP P1), DMA selection (black squares, EXP P6), and multi-charging correction (white squares). The red line represents the calculation simulating organic coated compounds at the AS particle surface using Eq. (3) with a surface density of 1.1×10^{-3} g m^{-2} (selected from Fig. 4).

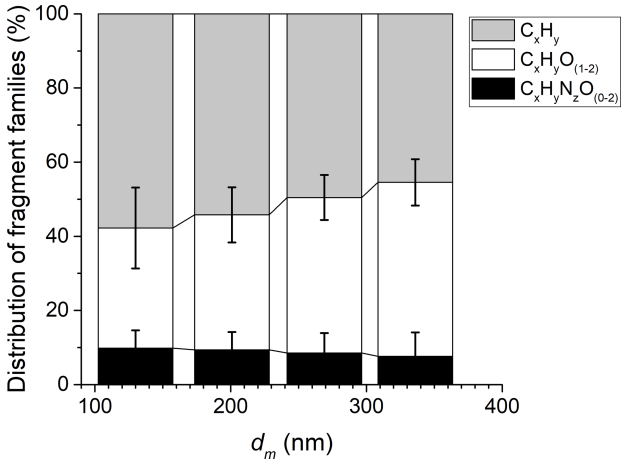

Figure 6. Mass fractions of the three main sets of organic fragments present in AS particles as measured by the HR-ToF-AMS during EXP P1. The error bars represent the standard deviation from averaging multiple measurements.

3.3 Influence of AAC and DMA on the organic content

Particle size selection is important in aerosol science especially when particle size influences the properties studied. In this work, both AAC and DMA were used to provide monodisperse AS aerosols. As a recent commercial instrument, AAC was used to select AS aerosols in most of the experiments. The effects of the concentric cylinder rotation speed of the AAC were tested in EXP P7. The results (Sect. S6 in the Supplement) demonstrate that the rotation speed does not affect [Org] / [Sulfate]. While the AAC selects particles using centrifugal force, the DMA selects particles by their electromobility. In the latter, the selected distribution is thus not exclusively monodispersed as it contains double- and triple-charged particles at the corresponding sizes. Correction of the multi-charge effect was successfully applied and is routine in aerosol size distribution determination (Petters, 2018; Wiedensohler et al., 2012). However, Fig. 4 shows that the larger the particle, the lower the content of the organic compounds. In this case, the multi-charged particles affect the organic quantification using the DMA and the AMS, so corrections are needed. In this work, we compared [Org] / [Sulfate] in AS particles selected by the DMA and by the AAC, respectively (Fig. 5).

In Fig. 5 the white squares represent the multi-charging corrections considering the hypothesis that organic compounds coat the surface of AS particles as shown in Sect. 3.2. Details of the multi-charging corrections are given in Sect. S7 in the Supplement. Briefly, the corrected [Org] / [Sulfate] by the multi-charged modes are systematically higher than the non-corrected values because the correction considers the total amounts of organic compounds and sulfate. Using the DMA selection after correction, [Org] / [Sulfate] is clearly inversely related to the mobility size and in very good agreement with those results obtained using the AAC selection. In conclusion, the intercomparison of the two instruments shows that the influence of the instrument is negligible, and it also shows that the selection by AAC leads to lower uncertainties on the y axis and therefore more accurate results.

3.4 Tentative identification of organic content

From the HR-ToF-AMS mass spectra, the three main families present in AS particles were C_xH_y, $C_xH_yO_{(1–2)}$, and $C_xH_yNO_{(0–2)}$. Figure 6 shows the proportion of these three groups relative to total organic compounds as a function of AS particle size. Within the uncertainties, the proportion of the three families remains constant and independent of the particle size, which shows the stability of the organic compounds coated on AS particles.

The identification of the corresponding organic compounds was limited by the high fragmentation due to the electron impact ionization operated in the HR-ToF-AMS instrument. Further identification was conducted by LC–MS with liquid AS solutions. In EXP C1 and C2, an aqueous solution of ammonium sulfate (99.5 %) at 1.5 M was injected and analyzed in the positive mode. The acetonitrile and methanol eluents showed similar results for compound separation. Figure 7 shows a chromatogram of an ammonium sulfate solution (green line) as well as blanks of Milli-Q water (red line) and Fisher water (blue line). In Milli-Q water, two ions were present at retention times of 4.45 and 4.65 min, and their mass spectra were attributed to nylon polymers $(C_6H_{11}NO)_n$ which are among the frequently reported interfering compounds (Tran and Doucette, 2006; Keller et al., 2008). However, no significant contamination was observed

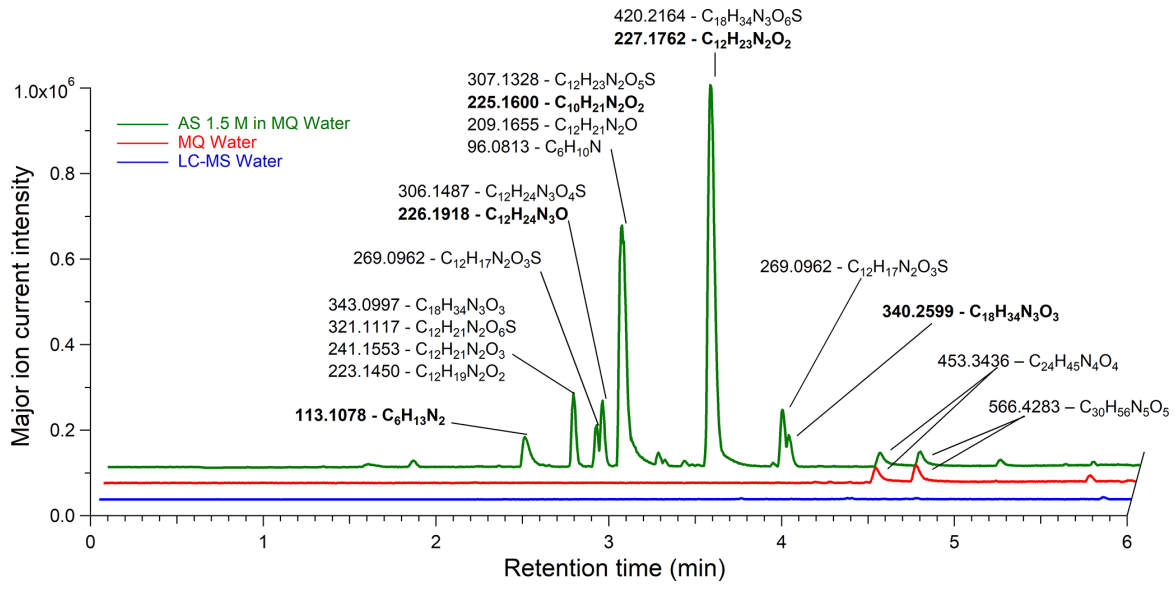

Figure 7. LC/ESI$^+$–MS base peak chromatogram of Milli-Q water, Fisher water, and AS (99.5 %) solution of 1.5 M (EXP C1) with corresponding major ion masses associated with raw formulas. The bold ion masses and proposed raw formula were studied in MS–MS (EXP C9). Ions displayed in boldface were detected in their $[M-H]^-$ form in LC/ESI$^-$–MS (in EXP C6–C8).

in the Fisher water (LC–MS Grade). Figure 7 shows that the same ions found in Milli-Q water were also present in the AS solution prepared in the same Milli-Q water. Many other ions were detected in the AS solution, and their retention times highly suggested that these molecules were organic. The proposed raw formulas systematically contained carbon, hydrogen, oxygen, nitrogen, and sometimes sulfur, consistent with the HR-ToF-AMS spectra. The double bond equivalence (DBE) varies from 1 to 5 showing that the molecules are unsaturated and potentially cyclic. Different to nylon polymers found in Milli-Q water, these raw formulas are not referenced among the common laboratory LC–MS contaminants (Keller et al., 2008). The mass error was always well below 5 ppm and no raw formula with a sodium adduct was suggested. Some of the m/z showed two different retention times, implying potentially the presence of isomers. For example, at m/z 226.1918, two peaks were detected, one at 2.89 min and the other at 3.11 min as described in detail in Sect. S8 in the Supplement for the most intense ions. In the negative ESI mode, the signal was overwritten by the sulfate ion (detected at $[M+H]^-$: 96.9596, HSO_4^-) along the whole chromatogram, due to the high ammonium sulfate concentrations used.

For further identification and for detection in the negative mode, AS crystals and solutions at various concentrations were extracted using different solvents and different methods (C3–C7 in Table 2). In the positive mode, more than 60 % of the molecules identified without the extraction step were also detected. Compared with other solvents, acetonitrile was found to be the most efficient extracting solvent. In the negative mode, the signal was systematically much lower (ion current intensity $< 10^3$ counts s^{-1}) and only molecules displayed in boldface in Fig. 7 were detected. Consequently, no further analysis was performed in the negative mode due to the low signal. In EXP C8 and C10, another brand of AS crystals of the same purity (99.5 %) was tested for comparison. Some common ions were detected in the extracts in the positive mode but at a much lower intensity (by a factor of ~ 20; see Sect. S9 in the Supplement), thus demonstrating that the detected organic compounds were present in both AS crystals and that the level of organic contamination depends at least in part on the AS brand. EMSURE® products are supposed to offer a high level of quality and appear to be less contaminated despite the same reported purity. Figure 8 shows the MS–MS measurements operated on two ions detected in EXP C9 (see Sect. S10 in the Supplement for the complete MS–MS results). These results support the proposed raw formula, confirming that these organic compounds contained oxygen and nitrogen and/or sulfur. They also show recurrent fragments: for instance, fragment ion at m/z 96.082, most likely described by the raw formula $C_6H_{10}N$, was found in all the MS–MS spectra as well as the fragment ion at m/z 69.072 corresponding to C_5H_9 which was also a fragment observed in the spectra from the HR-ToF-AMS with high intensity.

These results confirm that the organic compounds present in AS are large molecules: of the 20 most intense detected molecules, 12 contained 12 carbon atoms (C_{12}), and the others contained C_6 (2 molecules bearing $C_xH_yN_{1/2}$), C_{10} (1 molecule), C_{11} (1 molecule), C_{17} (1 molecule), C_{18} (2 molecules), and up to C_{24} (1 molecule), with m/z ranging from 96 to 533. Apart from the 2 smallest molecules (C_6),

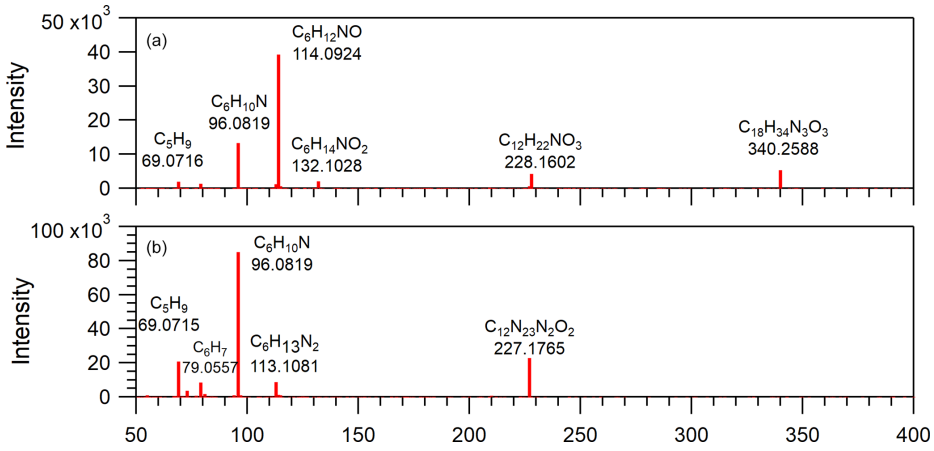

Figure 8. Mass spectra obtained from LC/ESI$^+$–MS/MS measurements of two detected compounds in EXP C9. The $[M+H]^+$ ions were detected at **(a)** m/z 340, using a collision energy of 25 eV, and **(b)** m/z 227, using a collision energy of 20 eV.

all of them bear mono- or poly-functional groups with at least 2 heteroatoms (N and O are always present, and S is found in 10 molecules) confirming their low volatility. Most of them fragment following the same scheme, thus showing similar structures. No structure is proposed here as there are many possible structures. The fact that these molecules were largely detected in the positive mode and that they all bear at least one N atom, and the fact that they were observed specifically at the surface of the AS aerosol particles, could suggest that they are cationic surfactants such as quaternary ammonium salts remaining from the manufacturing processes. Ammonium sulfate is typically produced by the reaction of gaseous ammonia with sulfuric acid, but the precise manufacturing processes and raw materials of the suppliers are not known in detail and therefore do not allow us to draw any conclusions for these processes.

3.5 Removing organic traces from AS aerosol particles

To give recommendations on the use of AS for laboratory studies or instrument calibrations with organic contaminations as low as possible, the results of EXP P2–P5 using high-quality water, and AS or purified AS crystals, are shown in Fig. 9 where [Org] / [Sulfate] is plotted versus particle size.

Figure 9 shows that, although decreasing with increasing purification, organic traces remain present in all experiments. They seem to remain coated at the surface of the particles, as shown by the good agreement between the simulations and experimental data. According to the simulation results, a reduction of 20 % of [Org] / [Sulfate] is observed when Fisher water (red squares) replaces Milli-Q water (pink triangles). This reduction might be due to the removal of nylon polymers found in Milli-Q water (Fig. 7). However, no significant difference is observed between EXP P2, P3, and P4, i.e., purification of AS crystals by acetonitrile or recrystallization is not efficient enough to remove organic traces. Finally, comparing EXP P5 (cyan triangles) and P2 (red squares), another

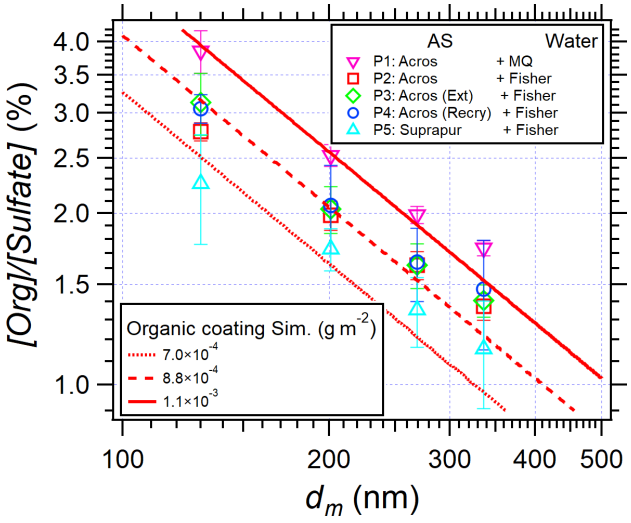

Figure 9. [Org] / [Sulfate] in AS aerosol particles as a function of mobility diameter in EXP P1–P5. The red lines represent the calculated [Org] / [Sulfate] simulating surface coating of organic matter (from Eq. 3) for EXP P1, P4, and P5.

20 % reduction of organic traces is observed when highly pure AS crystals are used (99.9999 %). In this case, the organic traces are lower than 2.5 % on the AS particles with $d_m = 130$ to 336 nm (corresponding to $d_a = 200$ to 500 nm).

4 Conclusions and implications

Ammonium sulfate is one of the dominant components of atmospheric aerosol and is widely used in laboratory experiments and for instrument calibration purposes. However, the widely used commercial AS crystals may contain interfering organic impurities. To answer questions related to the quantity and the quality of organic impurities found in widely

used commercial AS products, a series of experiments were performed to quantify and identify organic impurities on AS aerosol particles and in liquid solutions using an HR-ToF-AMS and LC–MS. The results showed that, using 99.5 % purity AS, up to 3.8 % of organic impurities were present related to sulfate mass. This ratio was found to be independent of the concentration of nebulized AS solutions but was inversely related to the particle size. The simulations of AS organic mixtures showed a homogeneous organic coating on the surface of AS particles with a constant surface density of $1.1 \times 10^{-3}\,\mathrm{g\,m^{-2}}$. Regarding the particle size selection system, the comparison between AAC and DMA showed consistent [Org] / [Sulfate], thus highlighting that the observed particle size effects were not due to instrumental artifacts. Using LC–MS analysis of the organic content showed up to 20 different stable, highly functionalized molecules with nitrate, amine, and/or sulfate groups. The proposed raw formulas included mostly C_{12} compounds with mono- or polyfunctional groups with at least two heteroatoms (N and O were always present, and S was found in 10 molecules) suggesting low volatility. These nitrogenous molecules were abundantly detected by LC–MS in AS solutions in the positive ESI mode, and in the nebulized solutions, they were observed to be coated on the surface of AS aerosol particles. Thus, it could be suggested that they might comprise cationic surfactants such as quaternary ammonium salts remaining from the manufacturing processes.

From this suggestion, the potential effects of organic impurities on CCN activation of AS aerosols were investigated to determine the error made on the critical supersaturation if one assumes 100 % AS, omitting the presence of organic impurities. This estimation was performed with a simple calculation using the κ-Köhler equation (Petters and Kreidenweis, 2007) (see Sect. S11 in the Supplement for details). For the estimation of the critical supersaturation in the presence of organic impurities, two extreme hypotheses were explored. In hypothesis 1, the organic fraction was considered soluble and non-surface-active, whereas in hypothesis 2, it was considered extremely surface-active, using the most powerful surfactant as a proxy. Following each of these hypotheses, the supersaturation was calculated along the droplet activation of an AS particle of 130 nm with and without organic impurities (Fig. S11 in the Supplement). The results show that whereas the critical supersaturation of AS aerosols is not significantly impacted by the presence of organic impurities under hypothesis 1, it is highly impacted under hypothesis 2, with a potential error of more than 70 %.

In view of these extreme results, and especially the very important error observed for surface-active compounds, the potential quantity of surface-active species contained in AS solutions (ammonium sulfate from Acros Organics, 99.5 % diluted in Milli-Q water) was investigated (Sect. S12 in the Supplement). The results showed that AS solutions contain extremely low amounts of cationic and non-ionic surfactants, and an upper limit of [Org surfactant] / [Sulfate] mass ratio of 1×10^{-5} % was determined. Although this ratio is five orders of magnitude lower than the total organic fraction detected in AS particles, the potential effect of these surfactants on the surface tension of 130 nm diameter AS particles was investigated. For such particles, the obtained [Org surfactant] / [Sulfate] mass ratio induces a concentration of $6 \times 10^{-7}\,\mathrm{mol\,L^{-1}}$ of surfactants. At this very low concentration, even the most surface-active molecules show a surface tension similar to that of pure water as shown by surface tension isotherms (Ekström et al., 2010; Frossard et al., 2019; Arabadzhieva et al., 2020). It was thus concluded that the CCN activity of AS particles with $d_\mathrm{m} = 130$ nm should not be significantly affected by the presence of the organic impurities. However, caution should be taken to keep their amounts as low as possible.

In this work, some efforts to remove these organic impurities have been tentatively tested by purifying and recrystallizing AS crystals. Though no significant difference was observed, it is likely that better results could be obtained by increasing the number of purification and recrystallization cycles, as very high purity AS crystals (99.9999 %) showed significantly lower organic content. It is therefore recommended to use AS seeds with caution, especially when small particles are used, in terms of AS purity and water purity when aqueous solutions are used for atomization.

Appendix A: Morphological properties of AS aerosols

Following the method of Zelenyuk et al. (2006), the shape factor (χ) in any flow regime (continuous and transient) can be determined by the ratio of $d_\mathrm{va}/d_\mathrm{m}$ in Eq. (A1):

$$\frac{d_\mathrm{va}}{d_\mathrm{m}} = \frac{\rho_\mathrm{p}}{\rho_0}\frac{1}{\chi^2}\frac{C_\mathrm{c}\left(d_\mathrm{va}\chi\rho_\mathrm{p}/\rho_0\right)}{C_\mathrm{c}\left(d_\mathrm{m}\right)}, \tag{A1}$$

where ρ_p is the particle density, ρ_0 is the standard density noticed as $1\,\mathrm{g\,cm^{-3}}$, and C_c is the Cunningham slip factor (Kim et al., 2005), given by Eq. (A2):

$$C_\mathrm{c}\left(K_\mathrm{n}\right) = 1 + K_\mathrm{n}\left[1.165 + 0.483\exp\left(-\frac{0.997}{K_\mathrm{n}}\right)\right]. \tag{A2}$$

$K_\mathrm{n}(d) = 2\lambda_\mathrm{g}/d$ is the Knudsen number, and λ_g is the gas mean free path. In this work, normal temperature and pressure (293.15 K at 1 atm) were applied for the calculation of the shape factor of AS aerosols.

The shape factor (χ) of monodisperse AS aerosols selected by the AAC was calculated according to Eq. (A1) and is shown in Table A1, together with the aerodynamic diameter (d_a) selected in the AAC, the mobility diameter d_m, and the vacuum aerodynamic diameter d_va representing the average mode of size distributions given by the SMPS and HR-ToF-AMS (p-ToF mode), respectively. Table A1 shows that, within the uncertainty, the selected AS particles own a size-independent shape factor of 1.06, which falls within the interval of 1.03 and 1.07 reported by Zelenyuk et al. (2006).

Table A1. Morphological properties of monodisperse AS aerosols selected by the AAC (in EXP P1 and P2): aerodynamic diameter (d_a), mobility diameter (d_m), vacuum aerodynamic diameter (d_{va}), and shape factor (χ). The uncertainty represents the standard deviation of several measurements under the same selection criteria.

d_a (nm)	d_m (nm)	d_{va} (nm)	Shape factor (χ)
200	126.6 ± 0.3	206 ± 6	1.05 ± 0.02
300	194.3 ± 0.3	312 ± 8	1.06 ± 0.02
400	267.6 ± 0.4	429 ± 10	1.06 ± 0.02
500	340.3 ± 0.4	539 ± 11	1.07 ± 0.02

Data availability. The data that are presented in this work are publicly available in the Zenodo public data repository at https://doi.org/10.5281/zenodo.6559283 (Wu et al., 2022).

Supplement. The supplement related to this article is available online at: https://doi.org/10.5194/amt-15-3859-2022-supplement.

Author contributions. JW and AM provided the initial idea for this work. JW and BTR performed the experiments and data analysis of AS aerosol characterization with the HR-ToF-AMS. NB and SR carried out the measurements of AS solutions with the LC–MS. JW, NB, and JLC proposed different purification processes of AS aerosols. The organic–inorganic mixing model was provided firstly by JW and improved by BR'M and AM. JW, NB, JMGS, and AM developed the structure of this paper. JW summarized all contributions and expressed them in this paper. All authors provided advice regarding improvements to this paper as well as to the writing of the final version of the manuscript.

Competing interests. The contact author has declared that neither they nor their co-authors have any competing interests.

Disclaimer. Publisher's note: Copernicus Publications remains neutral with regard to jurisdictional claims in published maps and institutional affiliations.

Acknowledgements. The authors acknowledge the support from the French National Research Agency (ANR-PRCI), as well as the French program CNRS-LEFE-CHAT (Programme National – Les Enveloppes Fluides et l'Environnement – Chimie Atmosphrique). The authors thank two colleagues, Jim Grisillon and Fabien Robert-Peillard, from the laboratory LCE – Aix Marseille University, who performed additional measurements for the quantification of surfactants in an AS solution. Finally, the authors acknowledge the first anonymous reviewer for her/his extremely thorough comments on the manuscript.

Financial support. This research has been supported by ANR-PRCI through the projects PARAMOUNT (grant no. ANR18-CE92-0038-02) and ORACLE (grant no. ANR-20-CE93-0008-01_ACT) and by CNRS-LEFE-CHAT through the project SURFACTs.

Review statement. This paper was edited by Hartmut Herrmann and reviewed by Angela Buchholz and one anonymous referee.

References

Abbatt, J. P. D., Broekhuizen, K., and Pradeep Kumar, P.: Cloud condensation nucleus activity of internally mixed ammonium sulfate/organic acid aerosol particles, Atmos. Environ., 39, 4767–4778, https://doi.org/10.1016/j.atmosenv.2005.04.029, 2005.

Aiken, A. C., DeCarlo, P. F., and Jimenez, J. L.: Elemental Analysis of Organic Species with Electron Ionization High-Resolution Mass Spectrometry, Anal. Chem., 79, 8350–8358, https://doi.org/10.1021/ac071150w, 2007.

Andreae, M. O. and Rosenfeld, D.: Aerosol–cloud–precipitation interactions. Part 1. The nature and sources of cloud-active aerosols, Earth-Sci. Rev., 89, 13–41, https://doi.org/10.1016/j.earscirev.2008.03.001, 2008.

Arabadzhieva, D., Tchoukov, P., and Mileva, E.: Impact of Adsorption Layer Properties on Drainage Behavior of Microscopic Foam Films: The Case of Cationic/Non-ionic Surfactant Mixtures, Colloids Interfaces, 4, 53, https://doi.org/10.3390/colloids4040053, 2020.

Badger, C. L., George, I., Griffiths, P. T., Braban, C. F., Cox, R. A., and Abbatt, J. P. D.: Phase transitions and hygroscopic growth of aerosol particles containing humic acid and mixtures of humic acid and ammonium sulphate, Atmos. Chem. Phys., 6, 755–768, https://doi.org/10.5194/acp-6-755-2006, 2006.

Brooks, S. D., DeMott, P. J., and Kreidenweis, S. M.: Water uptake by particles containing humic materials and mixtures of humic materials with ammonium sulfate, Atmos. Environ., 38, 1859–1868, https://doi.org/10.1016/j.atmosenv.2004.01.009, 2004.

Brüggemann, M., Xu, R., Tilgner, A., Kwong, K. C., Mutzel, A., Poon, H. Y., Otto, T., Schaefer, T., Poulain, L., Chan, M. N., and Herrmann, H.: Organosulfates in Ambient Aerosol: State of Knowledge and Future Research Directions on Formation, Abundance, Fate, and Importance, Environ. Sci. Technol., 54, 3767–3782, https://doi.org/10.1021/acs.est.9b06751, 2020.

Canagaratna, M. R., Jimenez, J. L., Kroll, J. H., Chen, Q., Kessler, S. H., Massoli, P., Hildebrandt Ruiz, L., Fortner, E., Williams, L. R., Wilson, K. R., Surratt, J. D., Donahue, N. M., Jayne, J. T., and Worsnop, D. R.: Elemental ratio measurements of organic compounds using aerosol mass spectrometry: characterization, improved calibration, and implications, Atmos. Chem. Phys., 15, 253–272, https://doi.org/10.5194/acp-15-253-2015, 2015.

Charlson, R. J., Schwartz, S., Hales, J., Cess, R. D., Coakley, J. J., Hansen, J., and Hofmann, D.: Climate forcing by anthropogenic aerosols, Science, 255, 423–430, 1992.

Clegg, S. L., Brimblecombe, P., and Wexler, A. S.: Thermodynamic Model of the System H^+-NH_4^+-Na^+-SO_4^{2-}-NO_3^--

Cl^--H_2O at 298.15 K, J. Phys. Chem. A, 102, 2155–2171, https://doi.org/10.1021/jp973043j, 1998.

Darer, A. I., Cole-Filipiak, N. C., O'Connor, A. E., and Elrod, M. J.: Formation and stability of atmospherically relevant isoprene-derived organosulfates and organonitrates, Environ. Sci. Technol., 45, 1895–1902, 2011.

DeCarlo, P. F., Slowik, J. G., Worsnop, D. R., Davidovits, P., and Jimenez, J. L.: Particle Morphology and Density Characterization by Combined Mobility and Aerodynamic Diameter Measurements. Part 1: Theory, Aerosol Sci. Technol., 38, 1185–1205, https://doi.org/10.1080/027868290903907, 2004.

DeCarlo, P. F., Kimmel, J. R., Trimborn, A., Northway, M. J., Jayne, J. T., Aiken, A. C., Gonin, M., Fuhrer, K., Horvath, T., Docherty, K. S., Worsnop, D. R., and Jimenez, J. L.: Field-Deployable, High-Resolution, Time-of-Flight Aerosol Mass Spectrometer, Anal. Chem., 78, 8281–8289, https://doi.org/10.1021/ac061249n, 2006.

De Haan, D. O., Hawkins, L. N., Welsh, H. G., Pednekar, R., Casar, J. R., Pennington, E. A., de Loera, A., Jimenez, N. G., Symons, M. A., Zauscher, M., Pajunoja, A., Caponi, L., Cazaunau, M., Formenti, P., Gratien, A., Pangui, E., and Doussin, J.-F.: Brown Carbon Production in Ammonium- or Amine-Containing Aerosol Particles by Reactive Uptake of Methylglyoxal and Photolytic Cloud Cycling, Environ. Sci. Technol., 51, 7458–7466, https://doi.org/10.1021/acs.est.7b00159, 2017.

Ekström, S., Nozière, B., Hultberg, M., Alsberg, T., Magnér, J., Nilsson, E. D., and Artaxo, P.: A possible role of ground-based microorganisms on cloud formation in the atmosphere, Biogeosciences, 7, 387–394, https://doi.org/10.5194/bg-7-387-2010, 2010.

Engelhart, G. J., Asa-Awuku, A., Nenes, A., and Pandis, S. N.: CCN activity and droplet growth kinetics of fresh and aged monoterpene secondary organic aerosol, Atmos. Chem. Phys., 8, 3937–3949, https://doi.org/10.5194/acp-8-3937-2008, 2008.

Frossard, A. A., Gérard, V., Duplessis, P., Kinsey, J. D., Lu, X., Zhu, Y., Bisgrove, J., Maben, J. R., Long, M. S., Chang, R. Y.-W., Beaupré, S. R., Kieber, D. J., Keene, W. C., Nozière, B., and Cohen, R. C.: Properties of Seawater Surfactants Associated with Primary Marine Aerosol Particles Produced by Bursting Bubbles at a Model Air–Sea Interface, Environ. Sci. Technol., 53, 9407–9417, https://doi.org/10.1021/acs.est.9b02637, 2019.

Gérard, V., Noziere, B., Fine, L., Ferronato, C., Singh, D. K., Frossard, A. A., Cohen, R. C., Asmi, E., Lihavainen, H., Kivekäs, N., Aurela, M., Brus, D., Frka, S., and Cvitešiæ Kušan, A.: Concentrations and Adsorption Isotherms for Amphiphilic Surfactants in PM1 Aerosols from Different Regions of Europe, Environ. Sci. Technol., 53, 12379–12388, https://doi.org/10.1021/acs.est.9b03386, 2019.

Grace, D. N., Lugos, E. N., Ma, S., Griffith, D. R., Hendrickson, H. P., Woo, J. L., and Galloway, M. M.: Brown Carbon Formation Potential of the Biacetyl–Ammonium Sulfate Reaction System, ACS Earth Space Chem., 4, 1104–1113, https://doi.org/10.1021/acsearthspacechem.0c00096, 2020.

Hämeri, K., Charlson, R., and Hansson, H.-C.: Hygroscopic properties of mixed ammonium sulfate and carboxylic acids particles, AIChE J., 48, 1309–1316, https://doi.org/10.1002/aic.690480617, 2002.

Hawkins, L. N., Welsh, H. G., and Alexander, M. V.: Evidence for pyrazine-based chromophores in cloud water mimics containing methylglyoxal and ammonium sulfate, Atmos. Chem. Phys., 18, 12413–12431, https://doi.org/10.5194/acp-18-12413-2018, 2018.

Hensley, J. C., Birdsall, A. W., Valtierra, G., Cox, J. L., and Keutsch, F. N.: Revisiting the reaction of dicarbonyls in aerosol proxy solutions containing ammonia: the case of butenedial, Atmos. Chem. Phys., 21, 8809–8821, https://doi.org/10.5194/acp-21-8809-2021, 2021.

Herrmann, H.: Kinetics of Aqueous Phase Reactions Relevant for Atmospheric Chemistry, Chem. Rev., 103, 4691–4716, https://doi.org/10.1021/cr020658q, 2003.

Hu, K. S., Darer, A. I., and Elrod, M. J.: Thermodynamics and kinetics of the hydrolysis of atmospherically relevant organonitrates and organosulfates, Atmos. Chem. Phys., 11, 8307–8320, https://doi.org/10.5194/acp-11-8307-2011, 2011.

Iinuma, Y., Müller, C., Berndt, T., Böge, O., Claeys, M., and Herrmann, H.: Evidence for the Existence of Organosulfates from â-Pinene Ozonolysis in Ambient Secondary Organic Aerosol, Environ. Sci. Technol., 41, 6678–6683, https://doi.org/10.1021/es070938t, 2007.

IPCC: Climate Change 2013 – The Physical Science Basis: Working Group I Contribution to the Fifth Assessment Report of the Intergovernmental Panel on Climate Change, edited by: Stocker, T. F., Qin, D., Plattner, G.-K., Tignor, M., Allen, S. K., Boschung, J., Nauels, A., Xia, Y., Bex, V., and Midgley, P. M., Cambridge University Press, Cambridge, https://doi.org/10.1017/CBO9781107415324, 2013.

Jimenez, J. L., Canagaratna, M. R., Donahue, N. M., Prevot, A. S. H., Zhang, Q., Kroll, J. H., DeCarlo, P. F., Allan, J. D., Coe, H., Ng, N. L., Aiken, A. C., Docherty, K. S., Ulbrich, I. M., Grieshop, A. P., Robinson, A. L., Duplissy, J., Smith, J. D., Wilson, K. R., Lanz, V. A., Hueglin, C., Sun, Y. L., Tian, J., Laaksonen, A., Raatikainen, T., Rautiainen, J., Vaattovaara, P., Ehn, M., Kulmala, M., Tomlinson, J. M., Collins, D. R., Cubison, M. J., E, Dunlea, J., Huffman, J. A., Onasch, T. B., Alfarra, M. R., Williams, P. I., Bower, K., Kondo, Y., Schneider, J., Drewnick, F., Borrmann, S., Weimer, S., Demerjian, K., Salcedo, D., Cottrell, L., Griffin, R., Takami, A., Miyoshi, T., Hatakeyama, S., Shimono, A., Sun, J. Y., Zhang, Y. M., Dzepina, K., Kimmel, J. R., Sueper, D., Jayne, J. T., Herndon, S. C., Trimborn, A. M., Williams, L. R., Wood, E. C., Middlebrook, A. M., Kolb, C. E., Baltensperger, U., and Worsnop, D. R.: Evolution of Organic Aerosols in the Atmosphere, Science, 326, 1525–1529, https://doi.org/10.1126/science.1180353, 2009.

Jimenez, N. G., Sharp, K. D., Gramyk, T., Ugland, D. Z., Tran, M.-K., Rojas, A., Rafla, M. A., Stewart, D., Galloway, M. M., Lin, P., Laskin, A., Cazaunau, M., Pangui, E., Doussin, J.-F., and De Haan, D. O.: Radical-Initiated Brown Carbon Formation in Sunlit Carbonyl–Amine–Ammonium Sulfate Mixtures and Aqueous Aerosol Particles, ACS Earth Space Chem., 6, 228–238, https://doi.org/10.1021/acsearthspacechem.1c00395, 2022.

Johnson, T. J., Irwin, M., Symonds, J. P. R., Olfert, J. S., and Boies, A. M.: Measuring aerosol size distributions with the aerodynamic aerosol classifier, Aerosol Sci. Technol., 52, 655–665, https://doi.org/10.1080/02786826.2018.1440063, 2018.

Kampf, C. J., Jakob, R., and Hoffmann, T.: Identification and characterization of aging products in the glyoxal/ammonium sulfate system – implications for light-absorbing material in

atmospheric aerosols, Atmos. Chem. Phys., 12, 6323–6333, https://doi.org/10.5194/acp-12-6323-2012, 2012.

Keller, B. O., Sui, J., Young, A. B., and Whittal, R. M.: Interferences and contaminants encountered in modern mass spectrometry, Anal. Chim. Acta, 627, 71–81, https://doi.org/10.1016/j.aca.2008.04.043, 2008.

Kiendler-Scharr, A., Mensah, A. A., Friese, E., Topping, D., Nemitz, E., Prevot, A. S. H., Äijälä, M., Allan, J., Canonaco, F., Canagaratna, M., Carbone, S., Crippa, M., Dall Osto, M., Day, D. A., De Carlo, P., Di Marco, C. F., Elbern, H., Eriksson, A., Freney, E., Hao, L., Herrmann, H., Hildebrandt, L., Hillamo, R., Jimenez, J. L., Laaksonen, A., McFiggans, G., Mohr, C., O'Dowd, C., Otjes, R., Ovadnevaite, J., Pandis, S. N., Poulain, L., Schlag, P., Sellegri, K., Swietlicki, E., Tiitta, P., Vermeulen, A., Wahner, A., Worsnop, D., and Wu, H.-C.: Ubiquity of organic nitrates from nighttime chemistry in the European submicron aerosol, Geophys. Res. Lett., 43, 7735–7744, https://doi.org/10.1002/2016GL069239, 2016.

Kim, J. H., Mulholland, G. W., Kukuck, S. R., and Pui, D. Y. H.: Slip Correction Measurements of Certified PSL Nanoparticles Using a Nanometer Differential Mobility Analyzer (Nano-DMA) for Knudsen Number From 0.5 to 83, J. Res. Natl. Inst. Stand. Technol., 110, 31–54, https://doi.org/10.6028/jres.110.005, 2005.

Kind, T. and Fiehn, O.: Seven Golden Rules for heuristic filtering of molecular formulas obtained by accurate mass spectrometry, BMC Bioinformatics, 8, 105, https://doi.org/10.1186/1471-2105-8-105, 2007.

King, S. M., Rosenoern, T., Shilling, J. E., Chen, Q., and Martin, S. T.: Increased cloud activation potential of secondary organic aerosol for atmospheric mass loadings, Atmos. Chem. Phys., 9, 2959–2971, https://doi.org/10.5194/acp-9-2959-2009, 2009.

Koehler, K. A., Kreidenweis, S. M., DeMott, P. J., Prenni, A. J., Carrico, C. M., Ervens, B., and Feingold, G.: Water activity and activation diameters from hygroscopicity data - Part II: Application to organic species, Atmos. Chem. Phys., 6, 795–809, https://doi.org/10.5194/acp-6-795-2006, 2006.

Laskin, J., Laskin, A., Nizkorodov, S. A., Roach, P., Eckert, P., Gilles, M. K., Wang, B., Lee, H. J., and Hu, Q.: Molecular Selectivity of Brown Carbon Chromophores, Environ. Sci. Technol., 48, 12047–12055, https://doi.org/10.1021/es503432r, 2014.

Meyer, N. K., Duplissy, J., Gysel, M., Metzger, A., Dommen, J., Weingartner, E., Alfarra, M. R., Prevot, A. S. H., Fletcher, C., Good, N., McFiggans, G., Jonsson, Å. M., Hallquist, M., Baltensperger, U., and Ristovski, Z. D.: Analysis of the hygroscopic and volatile properties of ammonium sulphate seeded and unseeded SOA particles, Atmos. Chem. Phys., 9, 721–732, https://doi.org/10.5194/acp-9-721-2009, 2009.

Moore, R. H., Ingall, E. D., Sorooshian, A., and Nenes, A.: Molar mass, surface tension, and droplet growth kinetics of marine organics from measurements of CCN activity, Geophys. Res. Lett., 35, L07801, https://doi.org/10.1029/2008GL033350, 2008.

Nandy, L. and Dutcher, C. S.: Phase Behavior of Ammonium Sulfate with Organic Acid Solutions in Aqueous Aerosol Mimics Using Microfluidic Traps, J. Phys. Chem. B, 122, 3480–3490, https://doi.org/10.1021/acs.jpcb.7b10655, 2018.

Nozière, B., Dziedzic, P., and Córdova, A.: Inorganic ammonium salts and carbonate salts are efficient catalysts for aldol condensation in atmospheric aerosols, Phys. Chem. Chem. Phys., 12, 3864–3872, https://doi.org/10.1039/B924443C, 2010.

Nozière, B., Baduel, C., and Jaffrezo, J.-L.: The dynamic surface tension of atmospheric aerosol surfactants reveals new aspects of cloud activation, Nat. Commun., 5, 3335, https://doi.org/10.1038/ncomms4335, 2014.

Ovadnevaite, J., Zuend, A., Laaksonen, A., Sanchez, K. J., Roberts, G., Ceburnis, D., Decesari, S., Rinaldi, M., Hodas, N., Facchini, M. C., Seinfeld, J. H., and O' Dowd, C.: Surface tension prevails over solute effect in organic-influenced cloud droplet activation, Nature, 546, 637–641, https://doi.org/10.1038/nature22806, 2017.

Petters, M. D.: A language to simplify computation of differential mobility analyzer response functions, Aerosol Sci. Technol., 52, 1437–1451, https://doi.org/10.1080/02786826.2018.1530724, 2018.

Petters, M. D. and Kreidenweis, S. M.: A single parameter representation of hygroscopic growth and cloud condensation nucleus activity, Atmos. Chem. Phys., 7, 1961–1971, https://doi.org/10.5194/acp-7-1961-2007, 2007.

Petters, M. D. and Kreidenweis, S. M.: A single parameter representation of hygroscopic growth and cloud condensation nucleus activity – Part 3: Including surfactant partitioning, Atmos. Chem. Phys., 13, 1081–1091, https://doi.org/10.5194/acp-13-1081-2013, 2013.

Pieber, S. M., El Haddad, I., Slowik, J. G., Canagaratna, M. R., Jayne, J. T., Platt, S. M., Bozzetti, C., Daellenbach, K. R., Fröhlich, R., Vlachou, A., Klein, F., Dommen, J., Miljevic, B., Jiménez, J. L., Worsnop, D. R., Baltensperger, U., and Prévôt, A. S. H.: Inorganic Salt Interference on CO_2^+ in Aerodyne AMS and ACSM Organic Aerosol Composition Studies, Environ. Sci. Technol., 50, 10494–10503, https://doi.org/10.1021/acs.est.6b01035, 2016.

Pöschl, U. and Shiraiwa, M.: Multiphase Chemistry at the Atmosphere–Biosphere Interface Influencing Climate and Public Health in the Anthropocene, Chem. Rev., 115, 4440–4475, https://doi.org/10.1021/cr500487s, 2015.

Powelson, M. H., Espelien, B. M., Hawkins, L. N., Galloway, M. M., and De Haan, D. O.: Brown Carbon Formation by Aqueous-Phase Carbonyl Compound Reactions with Amines and Ammonium Sulfate, Environ. Sci. Technol., 48, 985–993, https://doi.org/10.1021/es4038325, 2014.

Prenni, A. J., DeMott, P. J., and Kreidenweis, S. M.: Water uptake of internally mixed particles containing ammonium sulfate and dicarboxylic acids, Atmos. Environ., 37, 4243–4251, https://doi.org/10.1016/S1352-2310(03)00559-4, 2003.

Prisle, N. L.: A predictive thermodynamic framework of cloud droplet activation for chemically unresolved aerosol mixtures, including surface tension, non-ideality, and bulk–surface partitioning, Atmos. Chem. Phys., 21, 16387–16411, https://doi.org/10.5194/acp-21-16387-2021, 2021.

Saukko, E., Zorn, S., Kuwata, M., Keskinen, J., and Virtanen, A.: Phase State and Deliquescence Hysteresis of Ammonium-Sulfate-Seeded Secondary Organic Aerosol, Aerosol Sci. Technol., 49, 531–537, https://doi.org/10.1080/02786826.2015.1050085, 2015.

Seinfeld, J. H., Bretherton, C., Carslaw, K. S., Coe, H., DeMott, P. J., Dunlea, E. J., Feingold, G., Ghan, S., Guenther, A. B., Kahn, R., Kraucunas, I., Kreidenweis, S. M., Molina, M. J., Nenes, A., Penner, J. E., Prather, K. A., Ramanathan, V., Ramaswamy, V., Rasch, P. J., Ravishankara, A. R., Rosenfeld,

D., Stephens, G., and Wood, R.: Improving our fundamental understanding of the role of aerosol-cloud interactions in the climate system, P. Natl. Acad. Sci. USA, 113, 5781–5790, https://doi.org/10.1073/pnas.1514043113, 2016.

Shakya, K. M. and Peltier, R. E.: Non-sulfate sulfur in fine aerosols across the United States: Insight for organosulfate prevalence, Atmos. Environ., 100, 159–166, https://doi.org/10.1016/j.atmosenv.2014.10.058, 2015.

Sjogren, S., Gysel, M., Weingartner, E., Baltensperger, U., Cubison, M. J., Coe, H., Zardini, A. A., Marcolli, C., Krieger, U. K., and Peter, T.: Hygroscopic growth and water uptake kinetics of two-phase aerosol particles consisting of ammonium sulfate, adipic and humic acid mixtures, J. Aerosol Sci., 38, 157–171, https://doi.org/10.1016/j.jaerosci.2006.11.005, 2007.

Smith, M. L., You, Y., Kuwata, M., Bertram, A. K., and Martin, S. T.: Phase Transitions and Phase Miscibility of Mixed Particles of Ammonium Sulfate, Toluene-Derived Secondary Organic Material, and Water, J. Phys. Chem. A, 117, 8895–8906, https://doi.org/10.1021/jp405095e, 2013.

Sorjamaa, R., Svenningsson, B., Raatikainen, T., Henning, S., Bilde, M., and Laaksonen, A.: The role of surfactants in Köhler theory reconsidered, Atmos. Chem. Phys., 4, 2107–2117, https://doi.org/10.5194/acp-4-2107-2004, 2004.

Stokes, R. H. and Robinson, R. A.: Interactions in Aqueous Nonelectrolyte Solutions. I. Solute-Solvent Equilibria, J. Phys. Chem., 70, 2126–2131, https://doi.org/10.1021/j100879a010, 1966.

Surratt, J. D., Gómez-González, Y., Chan, A. W. H., Vermeylen, R., Shahgholi, M., Kleindienst, T. E., Edney, E. O., Offenberg, J. H., Lewandowski, M., Jaoui, M., Maenhaut, W., Claeys, M., Flagan, R. C., and Seinfeld, J. H.: Organosulfate Formation in Biogenic Secondary Organic Aerosol, J. Phys. Chem. A, 112, 8345–8378, https://doi.org/10.1021/jp802310p, 2008.

Szmigielski, R.: Evidence for C5 organosulfur secondary organic aerosol components from in-cloud processing of isoprene: Role of reactive SO_4 and SO_3 radicals, Atmos. Environ., 130, 14–22, https://doi.org/10.1016/j.atmosenv.2015.10.072, 2016.

Tavakoli, F. and Olfert, J. S.: An Instrument for the Classification of Aerosols by Particle Relaxation Time: Theoretical Models of the Aerodynamic Aerosol Classifier, Aerosol Sci. Technol., 47, 916–926, https://doi.org/10.1080/02786826.2013.802761, 2013.

Tervahattu, H., Hartonen, K., Kerminen, V.-M., Kupiainen, K., Aarnio, P., Koskentalo, T., Tuck, A. F., and Vaida, V.: New evidence of an organic layer on marine aerosols, J. Geophys. Res.-Atmos., 107, AAC 1-1–AAC 1-8, https://doi.org/10.1029/2000JD000282, 2002.

Trainic, M., Abo Riziq, A., Lavi, A., Flores, J. M., and Rudich, Y.: The optical, physical and chemical properties of the products of glyoxal uptake on ammonium sulfate seed aerosols, Atmos. Chem. Phys., 11, 9697–9707, https://doi.org/10.5194/acp-11-9697-2011, 2011.

Tran, J. C. and Doucette, A. A.: Cyclic polyamide oligomers extracted from nylon 66 membrane filter disks as a source of contamination in liquid chromatography/mass spectrometry, J. Am. Soc. Mass Spectrom., 17, 652–656, https://doi.org/10.1016/j.jasms.2006.01.008, 2006.

Treuel, L., Pederzani, S., and Zellner, R.: Deliquescence behaviour and crystallisation of ternary ammonium sulfate/dicarboxylic acid/water aerosols, Phys. Chem. Chem. Phys., 11, 7976–7984, https://doi.org/10.1039/B905007H, 2009.

Varutbangkul, V., Brechtel, F. J., Bahreini, R., Ng, N. L., Keywood, M. D., Kroll, J. H., Flagan, R. C., Seinfeld, J. H., Lee, A., and Goldstein, A. H.: Hygroscopicity of secondary organic aerosols formed by oxidation of cycloalkenes, monoterpenes, sesquiterpenes, and related compounds, Atmos. Chem. Phys., 6, 2367–2388, https://doi.org/10.5194/acp-6-2367-2006, 2006.

Vepsäläinen, S., Calderón, S. M., Malila, J., and Prisle, N. L.: Comparison of six approaches to predicting droplet activation of surface active aerosol – Part 1: moderately surface active organics, Atmos. Chem. Phys., 22, 2669–2687, https://doi.org/10.5194/acp-22-2669-2022, 2022.

Wach, P., Spólnik, G., Rudziñski, K. J., Skotak, K., Claeys, M., Danikiewicz, W., and Szmigielski, R.: Radical oxidation of methyl vinyl ketone and methacrolein in aqueous droplets: Characterization of organosulfates and atmospheric implications, Chemosphere, 214, 1–9, https://doi.org/10.1016/j.chemosphere.2018.09.026, 2019.

Wex, H., Petters, M. D., Carrico, C. M., Hallbauer, E., Massling, A., McMeeking, G. R., Poulain, L., Wu, Z., Kreidenweis, S. M., and Stratmann, F.: Towards closing the gap between hygroscopic growth and activation for secondary organic aerosol: Part 1 – Evidence from measurements, Atmos. Chem. Phys., 9, 3987–3997, https://doi.org/10.5194/acp-9-3987-2009, 2009.

Wiedensohler, A., Birmili, W., Nowak, A., Sonntag, A., Weinhold, K., Merkel, M., Wehner, B., Tuch, T., Pfeifer, S., Fiebig, M., Fjäraa, A. M., Asmi, E., Sellegri, K., Depuy, R., Venzac, H., Villani, P., Laj, P., Aalto, P., Ogren, J. A., Swietlicki, E., Williams, P., Roldin, P., Quincey, P., Hüglin, C., Fierz-Schmidhauser, R., Gysel, M., Weingartner, E., Riccobono, F., Santos, S., Grüning, C., Faloon, K., Beddows, D., Harrison, R., Monahan, C., Jennings, S. G., O'Dowd, C. D., Marinoni, A., Horn, H.-G., Keck, L., Jiang, J., Scheckman, J., McMurry, P. H., Deng, Z., Zhao, C. S., Moerman, M., Henzing, B., de Leeuw, G., Löschau, G., and Bastian, S.: Mobility particle size spectrometers: harmonization of technical standards and data structure to facilitate high quality long-term observations of atmospheric particle number size distributions, Atmos. Meas. Tech., 5, 657–685, https://doi.org/10.5194/amt-5-657-2012, 2012.

Wu, J., Brun, N., González-Sánchez, J. M., R'Mili, B., Temime Roussel, B., Ravier, S., Clément, J.-L., and Monod, A.: Raw data of article "Substantial organic impurities at the surface of synthetic ammonium sulfate particles", Zenodo [data set], https://doi.org/10.5281/zenodo.6559283, 2022.

Zelenyuk, A., Cai, Y., and Imre, D.: From Agglomerates of Spheres to Irregularly Shaped Particles: Determination of Dynamic Shape Factors from Measurements of Mobility and Vacuum Aerodynamic Diameters, Aerosol Sci. Technol., 40, 197–217, https://doi.org/10.1080/02786820500529406, 2006.